

Structure-activity relationship and mechanistic studies of bisaryl urea anticancer agents indicate mitochondrial uncoupling by a fatty acid-activated mechanism

Edward York¹, Daniel A. McNaughton², Ariane Roseblade¹, Charles G. Cranfield³, Philip A. Gale^{2,4}, Tristan Rawling^{1*}

¹School of Mathematical and Physical Sciences, Faculty of Science, University of Technology Sydney, Sydney, NSW, 2007, Australia;

²School of Chemistry, The University of Sydney, NSW, 2006, Australia;

³School of Life Sciences, Faculty of Science, University of Technology Sydney, Sydney, NSW, 2007, Australia;

⁴The University of Sydney Nano Institute (SydneyNano), The University of Sydney, NSW, 2006, Australia

* Corresponding author: Tristan Rawling, Tristan.Rawling@uts.edu.au

Abstract

Targeting the cancer cell mitochondrion is a promising approach for developing novel anticancer agents. The experimental anticancer agent **SR4** (*N,N'*-bis(3,5-dichlorophenyl)urea) induces apoptotic cell death in several cancer cell lines by uncoupling mitochondrial oxidative phosphorylation (OxPhos) using a protein free mechanism. However, the precise mechanism by which **SR4** depolarizes mitochondria is unclear because **SR4** lacks an acidic functional group typically found in protein-independent uncouplers. Recently it was shown that structurally related thioureas can facilitate proton transport across lipid bilayers by a fatty acid-activated mechanism, in which the fatty acid acts as the site of protonation/deprotonation and the thiourea acts as an anion transporter that shuttles deprotonated fatty acids across the phospholipid bilayer to enable proton leak. In this paper we show that **SR4**-mediated proton transport is enhanced by the presence of free fatty acids in the lipid bilayer, indicating that **SR4** uncouples mitochondria through the fatty acid-activated mechanism. This mechanistic insight was used to develop a library of substituted bisaryl ureas for structure-activity relationship (SAR) studies and subsequent cell testing. It was found that lipophilic electron-withdrawing groups on bisaryl ureas enhanced electrogenic proton transport via the fatty acid-activated mechanism, and capacity to depolarize mitochondria and reduce the viability of MDA-MB-231 breast cancer cells. The most active compound in the series reduced cell viability with greater potency than **SR4**, and was more effective at inhibiting ATP production.

Introduction

The discovery of cytotoxic agents that selectively target cancer cells is critical to the development of well-tolerated anticancer therapeutics. Cancer cell mitochondrion have emerged as a promising anticancer drug target because they are structurally and functionally distinct from mitochondria in non-cancerous cells and because of their central role in cellular metabolism and apoptosis.¹ Mitochondria are the site of oxidative phosphorylation (OxPhos), a process that converts nutrients into ATP. OxPhos commences in the mitochondrial matrix, the central region of mitochondria enclosed by the mitochondrial inner membrane (MIM), where nutrients are oxidized to form NADH and FADH₂. NADH and FADH₂ feed high energy electrons into the electron transport chain (ETC), a series of proteins embedded in the MIM. As electrons pass through the ETC protons are pumped from the matrix and into the intermembrane space, generating a proton gradient across the MIM. The resultant mitochondrial membrane potential ($\Delta\psi_M$) drives the flow of protons back into the matrix through the MIM-embedded protein ATP synthase, which catalyzes the formation of ATP.²⁻⁴ Thus, nutrient oxidation is coupled to ATP formation by the $\Delta\psi_M$. In cancer cells, deregulated mitochondrial metabolism results in a shift towards glycolysis and an increased mitochondrial $\Delta\psi_M$ compared to non-cancerous cells.⁵ Indeed, hyperpolarization of the MIM is a universal feature of cancer cells, and targeting $\Delta\psi_M$ may produce novel drugs that selectively target cancer cells.⁶⁻⁸

Mitochondrial uncouplers are compounds that uncouple nutrient oxidation from ATP production by collapsing the $\Delta\psi_M$.⁹ The most common uncouplers are protonophores, which are lipophilic weak acids that can shuttle protons across membranes such as the MIM via the protonophoric cycle (Figure 1a). The deprotonated uncoupler (A^-) accepts a proton in the intermembrane space and diffuses across the MIM in its neutral form ($A-H$). Deprotonation of the protonophore in the relatively alkaline matrix results in the transport of one proton across

the MIM. For the cycle to continue the deprotonated protonophore (A^-) must permeate the MIM and return to the intermembrane space, however this step is inhibited by the MIM's lipophilic core, which is relatively impermeable to anions.^{10,11} Thus, the acidic groups in protonophores are conjugated to extended π -systems, which provide a large surface area for delocalization of the anionic charge. Charge delocalization enhances the lipophilicity and MIM-permeability of the anionic protonophore and allows the cycle to continue.¹² Fatty acids such as palmitic acid are weak acids but poor protonophores because insufficient charge delocalization prevents the fatty acid carboxylate from permeating the MIM.^{13,14}

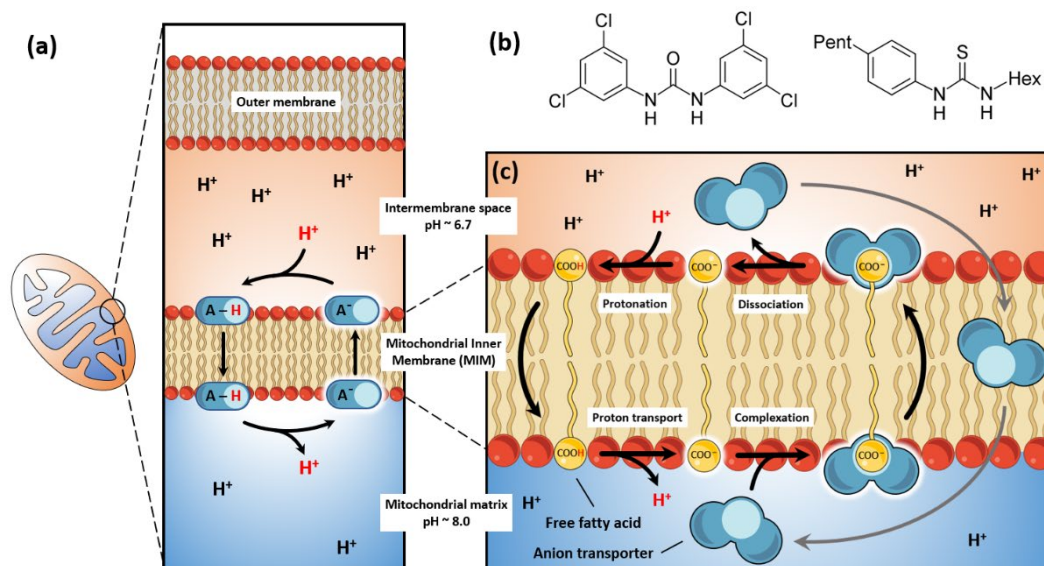


Figure 1 Proton transport and mitochondrial uncoupling by protonophoric and fatty acid-activated mechanisms (a) Mitochondrial uncoupling by classical protonophores. The protonophoric cycle that results in the transport of protons across the MIM and mitochondrial uncoupling. The rate determining step is diffusion of the anionic species across the MIM. To complete this step the negative charge is delocalized across an extended π -system to produce a MIM permeable anion. (b) Chemical structures of **SR4** and structurally related fatty acid-activated thiourea proton transporter respectively. (c) Fatty acid-activated proton transport mechanism. After deprotonation of the fatty acid in the mitochondrial matrix the thiourea-based

anion transporter binds carboxylate and masks the charge to facilitate fatty acid flip-flop and proton transport across the MIM.

The anticancer actions of mitochondrial uncouplers has been increasingly recognized as several uncouplers have been shown to selectively kill cancer cells.¹² One such compound is **SR4** (Figure 1b), a chlorinated bisaryl urea reported by Figarola *et al* to induce apoptotic cell death in leukaemia (HL-60), liver (HepG2) and lung (H358) cancer cells line *in vitro*.¹⁵⁻¹⁷ **SR4** also induces apoptosis in naïve and drug resistant melanoma (A375, SK-MEL-28) cell lines,¹⁸ and inhibits tumour growth in mouse models of cancer.¹⁷⁻¹⁹ Rigorous mechanistic studies established that **SR4** induces cell death through uncoupling of cancer cell mitochondria, and that uncoupling occurs by a protein-independent mechanism. However the precise mechanism by which **SR4**-mediated uncoupling occurs has not been determined because **SR4** lacks an acidic functional group required for protonophoric activity. Indeed, calculated and experimental pK_a values of substituted bisaryl ureas range from 14 to 18,²⁰ which is well above that of previously reported protonophores (pK_a values range from 4-8),⁹ and too high to allow protonation/deprotonation at mitochondrial pHs.

In 2016 Wu and Gale reported that thiourea-based anion receptors can mediate proton transport across lipid bilayers by a fatty acid-activated mechanism (Figure 1c), shown using unilamellar vesicles that model the MIM.²¹ Similar to the protonophoric cycle, the fatty acid carboxylate is protonated in the intermembrane space and permeates the MIM as a neutral species. Once in the alkaline matrix the fatty acid is deprotonated, which results in the transport of one proton and the formation of a fatty acid carboxylate that must diffuse back across the MIM. The thiourea next binds to the fatty acid carboxylate group through parallel hydrogen bonds with the thiourea NH groups, which masks the anionic charge to produce a complex that is sufficiently lipophilic to diffuse through the lipid bilayer. Dissociation in the intermembrane

space liberates the fatty acid and thiourea, allowing further proton transport to occur. Given that **SR4** is structurally similar to the thiourea-based anion receptors and aryl ureas are known anion receptors and transporters,²²⁻²⁵ and because the MIM contains free fatty acids,^{26,27} we suspected that **SR4** may uncouple mitochondria by the same fatty acid-activated mechanism. In this paper we show using a HPTS proton transport assay that **SR4**-mediated proton transport is enhanced by free fatty acids in the bilayer, indicating that **SR4** uncouples mitochondria through the fatty acid-activated mechanism. This insight was used to develop a library of substituted bisaryl ureas for structure-activity relationship (SAR) studies and subsequent cell testing. The resulting SAR demonstrated that lipophilic electron-withdrawing groups enhance fatty acid-activated proton transport, and analogues bearing these groups were found to effectively depolarize mitochondria and reduce cell viability in MDA-MB-231 breast cancer cells. The most potent transporter in the series (compound **3**) maintained the cellular actions of **SR4** and was found to uncouple mitochondrial OxPhos and impair ATP production.

RESULTS AND DISCUSSION

SR4-mediated proton transport is enhanced in phospholipid bilayers containing oleic acid

To determine if **SR4** can participate in the fatty acid-activated proton transport mechanism identified by Wu and Gale²¹ we used a similar HPTS fluorescence assay to measure electrogenic proton transport in large unilamellar 1-Palmitoyl-2-oleoyl-sn-glycero-3-phosphocholine (POPC) vesicles (200 nm) in HEPES-buffered potassium gluconate (100 mM) (Figure 2a, see Supporting Information for details).²⁸ In this system a pH gradient is established between the interior and exterior environments of the vesicles and proton transport is measured by monitoring the increase in intravesicular pH using the pH-sensitive fluorescent probe 8-hydroxypyrene-1, 3, 6-trisulfonic acid (HPTS). **SR4**-mediated proton transport was tested under three conditions, in untreated POPC vesicles, vesicles pretreated with bovine serum

albumin (BSA, 1 mol%) and vesicles pretreated with both BSA (1 mol%) and oleic acid (OA, 10 mol%), corresponding to 4 mol% free concentration after BSA binding). Pretreatment with BSA removes contaminating fatty acids present in POPC to detect proton transport via protonophoric cycling (i.e. classical protonophores). The addition of OA reintroduces the fatty acid-activated mechanism of proton transport, and any enhancement in activity can be assigned to this pathway.

As shown in Figure 2b, **SR4**-mediated proton transport is diminished in vesicles containing BSA compared to untreated vesicles, demonstrating that direct protonophoric cycling cannot explain the observed proton transport facilitated by **SR4**. This was anticipated because **SR4** lacks a functional group sufficiently acidic for deprotonation at mitochondrial pHs, and the slight efflux observed may be attributed to the traces of fatty acids that remain in the membrane after BSA treatment.²¹ Further, proton transport was enhanced in the presence of OA suggesting a fatty acid-dependent pathway. Combined these data indicate **SR4**-mediated proton transport across lipid bilayers is enhanced by free fatty acids, and is consistent with the hypothesis that **SR4** can act as a fatty acid-activated proton transporter.

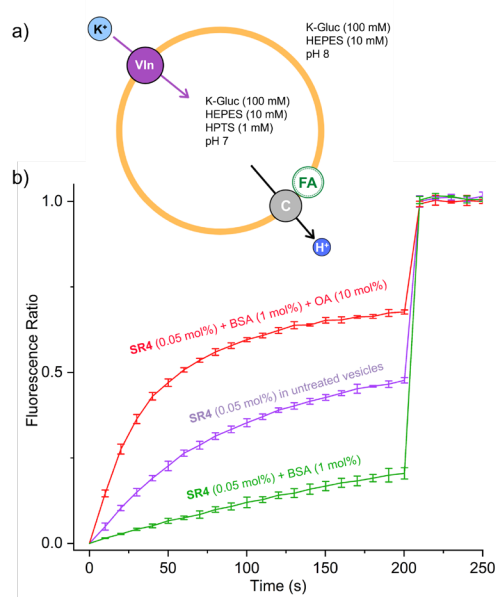
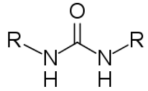
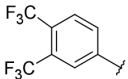
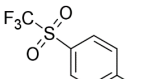
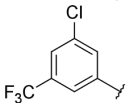
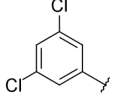
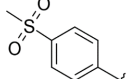
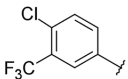
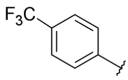
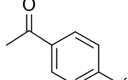
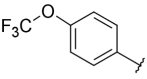
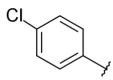
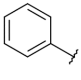
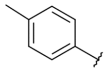
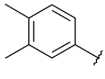
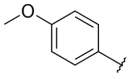


Figure 2 a) Schematic of the HTPS proton transport assay, monitored by HPTS fluorescence, outlining the conditions of the experiment and b) the proton transport induced by **SR4** under the various assay conditions. Vesicles were lysed at 200 s to provide a 100% dissipation reading for calibration purposes. Compound concentrations are represented as compound-to-lipid molar ratios.

Compound library design and synthesis

We next prepared a series of symmetrically substituted bisaryl ureas to determine if the observed SAR was consistent with the fatty acid-activated proton transport mechanism. Under this mechanism, the urea-based anion receptor promotes transbilayer movement (“flip-flop”) of anionic fatty acids by binding to and masking the carboxylate charge through parallel hydrogen bonds with the urea N-H groups, producing a complex that is sufficiently lipophilic to permeate lipid bilayers. It was anticipated that electron-withdrawing substituents on the bisaryl urea rings would enhance the carboxylate affinity of the urea binding group, promoting complexation and thus proton transport activity. It was also anticipated that lipophilic substituents would increase complex lipophilicity and improve activity. To test this a series of symmetrically substituted bisaryl ureas bearing substituents with various electron-withdrawing and donating capacities (determined from Hammett substituent constant, σ) and lipophilic properties (determined from hydrophobicity constant, π) were synthesized (Table 1). The compounds were synthesized in one step by reaction of *N,N'*-carbonyldiimidazole (CDI) with appropriately substituted anilines.

Table 1 Chemical structures, aromatic substituent constants, HPTS (200 s) EC₅₀ concentrations and Hill coefficients in untreated POPC vesicles, MTS (72 h) and JC-1 (1 h) absolute IC₅₀ concentrations measured in MDA-MB-231 breast cancer cells.

Compound	R	σ_{total}^a	π_{total}^a				
				HPTS EC ₅₀ (mol%)	Hill (n)	MTS IC ₅₀ (μM)	JC-1 IC ₅₀ (μM)
1		1.94	3.52	0.022 ± 0.001	0.91 ± 0.06	0.51 ± 0.1	1.80 ± 0.3
2		1.92	1.10	0.044 ± 0.002	1.38 ± 0.06	0.44 ± 0.1	2.34 ± 0.2
3		1.60	3.18	0.0046 ± 0.0004	0.82 ± 0.07	0.37 ± 0.1	0.26 ± 0.1
SR4		1.48	2.84	0.015 ± 5 x 10 ⁻⁴	1.01 ± 0.04	1.10 ± 0.3	0.45 ± 0.1
5		1.44	-3.26	- ^b	- ^b	- ^d	- ^d
6		1.32	3.18	0.010 ± 9 x 10 ⁻⁴	0.81 ± 0.1	0.68 ± 0.1	1.24 ± 0.3
7		1.08	1.76	0.023 ± 0.001	1.16 ± 0.06	0.84 ± 0.1	2.26 ± 0.4
8		1.00	-1.10	1.61 ± 0.04	1.15 ± 0.05	>100 ^c	22.9 ± 0.4
9		0.70	2.08	0.028 ± 0.005	1.33 ± 0.3	>100 ^c	>100 ^c
10		0.46	1.42	0.11 ± 0.03	2.00 ± 0.6	- ^d	>100 ^c
11		0	0	- ^b	- ^b	>100 ^c	>100 ^c
12		-0.34	1.12	- ^b	- ^b	- ^d	- ^d
13		-0.48	2.24	- ^b	- ^b	- ^d	- ^d
14		-0.54	-0.04	- ^b	- ^b	- ^d	- ^d

^a Aromatic substituent constants were taken from published values.²⁹ ^b Did not exceed 50 % efflux after 200 s at a loading of 10 mol%. ^c Produced moderate activity at 100 μM but insufficient for absolute IC₅₀ determination. ^d No activity observed at the maximum test concentration of 100 μM

Bisaryl ureas mediate proton transport by a fatty acid-activated mechanism

We first studied the ability of bisaryl ureas **1–14** to mediate electrogenic proton transport using the HPTS proton transport assay as performed for **SR4**. Dose-response studies and Hill analyses were performed for compounds **1–14** under three test conditions. An EC₅₀ value, which represents the concentration required to facilitate 50% of the maximum transport, and a Hill coefficient (n), which provides an indication of the stoichiometry of test compound required for the transport process, was calculated for each compound. Initially, the proton transport capability of compounds **1–14** were assessed in untreated vesicles to establish an SAR for the series (Table 1). Subsequently, dose-response studies were performed in the presence of BSA (1 mol%) or in the presence of both BSA (1 mol%) and OA (10 mol%) (Table 2).

Bisaryl ureas **1–SR4** and **6–10** achieved appreciable proton transport below 10 mol% loadings (compound-to-lipid molar ratio) such that EC₅₀ values could be calculated. The remaining compounds at commensurate concentrations did not exhibit significant activity, and higher loadings caused the compounds to precipitate out of aqueous media during experimental runs, meaning EC₅₀ values for the remaining compounds could not be calculated and were considered as inactive.

The SAR elicited from the HPTS assay data of the compounds in untreated vesicles indicates that lipophilic and electron-withdrawing substituents enhance electrogenic proton transport activity. The impact of electron-withdrawing capacity is highlighted clearly as compounds possessing electron-withdrawing substituents all showed appreciable activity apart from urea **5**, whereas compounds bearing electron-donating substituents (**12**, **13** and **14**), as well as the unsubstituted urea **11**, lacked activity. The importance of lipophilicity can be seen by comparison of urea **2** and **5**. Both compounds share similar electronic and steric properties, but differ substantially in lipophilicity. Bisaryl urea **2** is substituted with lipophilic

trifluoromethylsulfonyl groups and exhibited an EC₅₀ of 0.044 mol%. In contrast, while the hydrophilic methanesulfonyl groups of **5** are sufficiently electron-withdrawing, urea **5** lacked activity; presumably because it does not form fatty acid complexes with the lipophilicity required to permeate the lipid bilayer. That polar substituents reduce activity is also supported by urea **8**, which has electron-withdrawing but polar acetyl substituents and was found to be the least potent of the active compounds with an EC₅₀ of 1.61 mol%.

Compounds with two substituents generally outperformed those with a single *para* positioned electron-withdrawing group. Bisaryl urea **3** was the most potent proton transporter of the series, with an EC₅₀ value of 0.0046 mol%. **3** closely resembles the structure of **SR4**, bearing a trifluoromethyl group in place of a chlorine, however, its three-fold greater transport activity highlight that modest changes in lipophilic and electronic properties have significant effects on transport activity. However, notably urea **1** was less effective in the HPTS assays than compounds **3** and **6**, despite the replacement of a second chlorine with another trifluoromethyl substituent. Previous studies by the Gale group and others have highlighted that an optimal degree of lipophilicity is crucial for efficient transport activity.^{30,31} Compounds that are too lipophilic tend to localize in the non-polar interior of the lipid bilayer and struggle to diffuse into the aqueous phase to complete the transport cycle, resulting in diminished activity.

The EC₅₀ values determined under the BSA and BSA + OA experimental conditions are displayed in Table 2. Enhancement of transport activity in the presence of fatty acid was quantified using an activation factor, calculated by dividing the EC₅₀ in the presence of BSA by the EC₅₀ in the presence of both BSA and OA.²¹ An activation factor greater than 1 was returned for all compounds with appreciable activity, indicating that dissipation of the proton gradient is enhanced in the presence of fatty acid and, therefore, that the fatty acid-activated mechanism is the dominant pathway of proton transport for the active bisaryl urea compounds.

Table 2 HPTS EC₅₀ (200 s) concentrations and Hill coefficients in POPC vesicles in the presence of BSA and both BSA and OA.

Compound	EC ₅₀ (BSA)	n (BSA)	EC ₅₀ (OA)	n (OA)	Activation Factor ^a
1	0.065 ± 0.003	1.06 ± 0.05	0.014 ± 0.002	0.55 ± 0.1	4.64
2	0.044 ± 0.003	1.26 ± 0.2	0.033 ± 0.001	1.55 ± 0.05	1.33
3	0.06 ± 0.004	1.24 ± 0.09	0.003 ± 1 x 10 ⁻⁴	0.80 ± 0.04	20.00
SR4	0.075 ± 0.009	1.32 ± 0.2	0.00512 ± 4 x 10 ⁻⁴	1.36 ± 0.30	14.65
5	_ b	_ b	_ b	_ b	_ c
6	0.098 ± 0.004	1.04 ± 0.1	0.0040 ± 1 x 10 ⁻⁴	1.03 ± 0.03	24.50
7	0.13 ± 0.02	2.00 ± 0.4	0.012 ± 7 x 10 ⁻⁴	1.04 ± 0.03	10.83
8	_ b	_ b	0.63 ± 0.07	1.05 ± 0.10	_ c
9	0.35 ± 0.05	1.56 ± 0.3	0.019 ± 3 x 10 ⁻⁴	1.27 ± 0.03	18.42
10	_ b	_ b	0.042 ± 0.004	1.46 ± 0.20	_ c
11	_ b	_ b	_ b	_ b	_ c
12	_ b	_ b	_ b	_ b	_ c
13	_ b	_ b	_ b	_ b	_ c
14	_ b	_ b	_ b	_ b	_ c
CCCP²¹	0.0013	0.97	0.0014	0.99	0.93

^a EC₅₀ in the presence of BSA divided by EC₅₀ in the presence of both BSA and OA. ^b Did not exceed 50% efflux after 200 s at a loading of 10 mol%. ^c Activation factor could not be calculated.

proton transport facilitated by this compound occurs independently of fatty acids present in the membrane. Notably, urea **2** exhibited only mild activation in the presence of OA and was 10 times less potent than **3**, which may be attributed to its markedly lower lipophilicity compared to **3**. Hill analyses of compounds **8** and **10** for the HPTS assay in the presence of BSA could not be completed due to a lack of transport activity below 10 mol% loading. However, EC₅₀ values could be determined in the presence of OA, and were much lower than the 10 mol% thresholds (0.63 and 0.042 mol%, respectively). This further emphasizes the contribution of the fatty acid-activated mechanism as the main

Mitochondrial actions of bisaryl ureas 1-14

We next assessed the capacity of bisaryl ureas **1–14** to transport protons across the MIM and depolarize mitochondria in MDA-MB-231 cells using the JC-1 assay. JC-1 is a fluorescent cationic dye that partitions between the mitochondrial matrix and the cytosol according to the $\Delta\Psi_M$. In polarized mitochondria with high $\Delta\Psi_M$, JC-1 accumulates in the matrix and forms aggregates that fluoresce red. Upon dissipation of $\Delta\Psi_M$ by mitochondrial uncouplers, JC-1 diffuses into the cytosol and disaggregates into monomers that fluoresce green. Thus, the JC-1 red : green fluorescence ratio is proportional to the proton gradient across the MIM. JC-1 IC₅₀ concentrations for the ureas were determined from dose-response curves as the concentration required to shift the red : green fluorescence ratio by 50% of control (Table 1). One hour treatments were used to distinguish the direct actions of the bisaryl ureas on the MIM from the collapse of the $\Delta\Psi_M$ that occurs during apoptotic cell death.

The observed JC-1 activity was consistent with the SAR established from the HPTS assay. Analogues that induced mitochondrial depolarization with the lowest JC-1 IC₅₀ concentrations (**1**, **2**, **3**, **6**, **7** and **SR4**) were substituted with lipophilic and electron-withdrawing groups. Polar electron-withdrawing substituents reduced JC-1 activity, as reflected by the inactive urea **5** and urea **8**, which had a relatively high IC₅₀ of $22.9 \pm 0.4 \mu\text{M}$. The JC-1 results for these analogues follow the HPTS activity trends, and bivariate analysis using log reciprocal transformations of JC-1 IC₅₀ and HPTS EC₅₀ concentrations demonstrates a strong positive relationship ($r^2 = 0.87$, Supporting Figure S2). Ureas **9** and **10**, which both possess moderately electron-withdrawing substituents ($\sigma_{\text{total}} \leq 0.70$) in *para* positions, lacked sufficient activity when tested at their solubility limits to calculate JC-1 IC₅₀ concentrations. These analogues were active in HPTS assays, and the differences may arise from confounding factors (plasma membrane permeability, metabolic stability etc.) in cell-based assays that are not present in the cell free HPTS assay. Unsubstituted urea **11** and ureas substituted with electron-donating groups (**12**, **13** and **14**) had poor or no observable activity in both JC-1 and HPTS assays. Taken

together, these data support the hypothesis that, like **SR4**, active bisaryl ureas depolarize mitochondria by the fatty acid-activated mechanism.

Proton transport across the MIM by **SR4** leads to mitochondrial uncoupling and reductions in intracellular ATP. To confirm that the most potent urea **3** also produces these actions, we examined each one of these steps.

First we established that **3** was a mitochondrial uncoupler using the Seahorse Mito Stress test, which measures the oxygen consumption rate (OCR) of MDA-MB-231 cells. Treatment of the cells with the ATP synthase inhibitor oligomycin reduces electron flow through the ETC and lowers OCR. Addition of an uncoupler in these conditions collapses the proton gradient across the MIM and allows unimpeded ETC activity that is observed as an increase in OCR.³² As shown in Figure 3, addition of **3** (5 μ M), **SR4** (5 μ M) and the classical uncoupler FCCP (0.5 μ M) increased OCR in MDA-MB-231 cells treated with oligomycin, indicating that **3**, like **SR4** and FCCP, is a mitochondrial uncoupler. In contrast, urea **12** (10 μ M) failed to increase OCR, which was anticipated based on its inactivity in the HPTS and JC-1 assays.

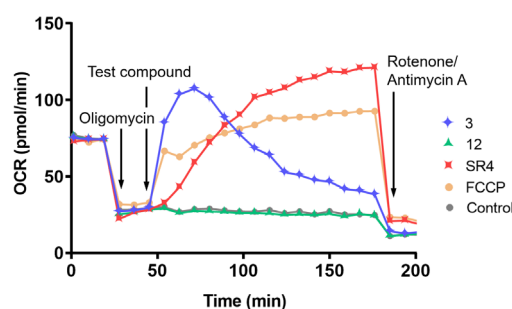


Figure 3 OCR in MDA-MB-231 cells treated sequentially with the ATP synthase inhibitor oligomycin (1 μ M), a test compound (5 μ M **SR4**, 5 μ M **3** or 10 μ M **12**), and the ETC complex inhibitors rotenone / antimycin A (1 μ M). Test compounds were compared against the classical protonophore FCCP (0.5 μ M) and a 0.1% DMSO vehicle containing no test compound as control.

ATP production by OxPhos is dependent on the proton gradient across the MIM, and collapse of the $\Delta\psi_M$ by mitochondrial uncouplers inhibits ATP production. We therefore assessed the effects of **SR4** and **3** on intracellular ATP levels in MDA-MB-231 cells. The uncoupler FCCP was included for comparison. Similar to previous observations in liver carcinoma (HepG2) and melanoma (A375 and MeWo) cell lines,^{15,18} **SR4** and FCCP both reduced intracellular ATP levels to ~85% of DMSO-treated control cells over eight hours (Figure 4). Urea **3** had the largest impact on intracellular ATP and reduced ATP levels to 60% of control after eight hours. The higher activity of **3** in this assay is consistent with the higher potencies observed for **3** in the HPTS and JC-1 assays. To confirm that the observed decreases in intracellular ATP were not a result of cell death LDH release assays were performed. These assays showed that **SR4** and **3** did not increase LDH release in MDA-MB-231 cells compared to control following 8 hours treatment (Supporting Figure S6), supporting the conclusion that **SR4** and **3** inhibit ATP production. Taken together, these data demonstrate that urea **3** produces similar cellular actions to **SR4** in MDA-MB-231 cells by depolarizing mitochondria, uncoupling OxPhos and inhibiting ATP production.

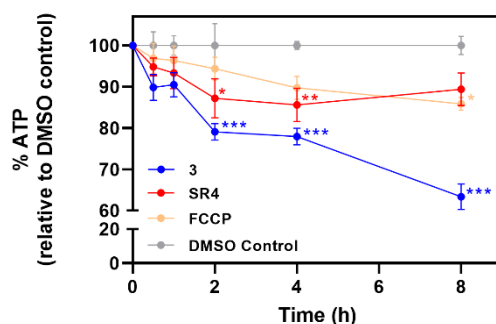


Figure 4 Total intracellular ATP levels in MDA-MB-231 cells following treatment with 5 μ M of **SR4**, **3**, FCCP or vehicle (DMSO) control. ATP levels are expressed as percentage of time-matched DMSO control. Different from DMSO-treated control: (*) $P < 0.05$, (**) $P < 0.01$, (***) $P < 0.001$.

Effects of bisaryl ureas 1-14 on MDA-MB-231 cell viability

Mitochondrial uncoupling by **SR4** is reported to lead to reduction in cancer cell viability,^{15,18} so we last assessed the effects of **1-14** on MDA-MB-231 cell viability using MTS assays, and compared the findings to the observed SAR from the HPTS and JC-1 data. Dose-response curves (Supporting Figure S3) were constructed from three independent repeats and used to calculate absolute IC₅₀ concentrations (Table 1). **SR4** reduced MDA-MB-231 cell viability with an IC₅₀ of 1.1 ± 0.3 μ M after 72 hours treatment, which is comparable to IC₅₀ concentrations reported against human HL-60 (1.2 μ M, 72 h MTT), HepG2 (3.5 μ M, 48 h MTT) and A2058 (5.0 μ M, 96 h MTT) cancer cell lines.¹⁵⁻¹⁷ Analogues **1**, **2**, **3**, **6** and **7** reduced MDA-MB-231 cell viability with absolute IC₅₀ concentrations between 0.3–1 μ M. Ureas **8** and **9** reduced cell viability at concentrations above 10 μ M, however absolute IC₅₀ concentrations could not be calculated for these compounds as they failed to reduce cell viability to below 50% of control. This activity could indicate these analogues impact cell viability by affecting progression through the cell cycle, an effect that has been demonstrated for **SR4**.^{15,16} All other bisaryl ureas were essentially inactive, with **11** producing only a moderate reduction in cell viability at the highest test concentration of 100 μ M.

Unlike the HPTS data, the MTS IC₅₀ concentrations calculated for the active compounds were all tightly grouped between 0.37 and 1.10 μ M, and the correlation observed between the JC-1 and HPTS results was not found between MTS IC₅₀ data and HPTS EC₅₀ data (Supporting Figure S4). One possible explanation is that some of the ureas in the series may be capable of inducing cell death by a second mechanism. For example, pyrimidine-based synthetic anion transporters transport chloride across cellular membranes, and have been shown to disrupt intracellular ion homeostasis and induce apoptotic cell death in HeLa and A549 cancer cell lines.³³ Despite this, broad similarities between HPTS and MTS activity remain. All analogues that displayed sufficient activity to calculate absolute MTS IC₅₀

concentrations (**1**, **2**, **3**, **6**, **7** and **SR4**) were substituted with lipophilic electron-withdrawing groups and exhibited proton transport activity in the HPTS assays. Urea **3** was the most active in the series in HPTS, JC-1 and MTS assays and was ~2–3 fold more active than **SR4** across all three assays. All analogues that lacked proton transport activity in HPTS assays (**5**, **11–14**) did not significantly reduce cell viability, and were unsubstituted or substituted with polar and/or electron-donating substituents.

Taken together, the data presented in this paper indicate that bisaryl ureas substituted with lipophilic electron-withdrawing groups uncouple mitochondria by the fatty acid-activated mechanism first identified by Wu and Gale,²¹ and that this uncoupling contributes to the ability of these compounds to reduce cancer cell viability.

Conclusions

In this paper we provide experimental evidence that **SR4** uncouples mitochondria by a fatty acid-activated proton transport mechanism first identified by Wu and Gale. Lipophilic and electron-withdrawing substituents on the bisaryl urea scaffold were shown to enhance electrogenic proton transport using this mechanism, promoting mitochondrial depolarization and reducing cell viability in MDA-MB-231 cells. The SAR is consistent with the proposed fatty acid-activated proton transport mechanism whereby bisaryl ureas facilitate fatty acid flip-flop by binding to fatty acid carboxylate groups to form MIM-permeable complexes. The most potent analogue **3**, like **SR4**, was shown to uncouple mitochondrial OxPhos and inhibit ATP formation in MDA-MB-231 breast cancer cells.

METHODS

Chemistry

CDI, 4-chloro-3-(trifluoromethyl) and 4-(methylsulfonyl)aniline was purchased from Fluorochem, aniline from Univar and 3,4-bis(trifluoromethyl)aniline from Combiblocks. The remaining substituted anilines were purchased from Sigma Aldrich. Reactions were monitored using TLC on Merck silica gel 60 F₂₅₄ aluminium backed plates. ¹H NMR (500 MHz) and ¹³C NMR (125 MHz) spectra were recorded using an Agilent 500 MHz NMR spectrometer. Spectra were referenced internally to residual solvent (DMSO-*d*₆: ¹H δ 2.50, ¹³C δ 39.52). Melting point determination was performed using a Gallenkamp melting point apparatus. High resolution mass spectra (HRMS) were recorded on an Agilent Technologies 6510 Q-TOF LCMS. The purity of all test compounds was confirmed to be >95% by absolute quantitative NMR spectroscopy (Supporting Table S1).

General bisaryl urea synthesis

N,N'-carbonyldiimidazole (1.0 mmol) was added to a solution of substituted aniline (2.0 mmol) in anhydrous dichloromethane (DCM, 5 ml) under a nitrogen atmosphere. The solution was refluxed until TLC indicated complete consumption of the aniline (6-48 hours). The products were purified by one of the following methods:

Method A: The product formed a precipitate in the reaction mixture that was isolated by vacuum filtration and washed with DCM. Any unreacted aniline was then removed by trituration with 1M HCl (3 x 5 ml).

Method B: The reaction mixture was washed with brine, dried over MgSO₄ and concentrated under reduce pressure. The resulting solid was triturated with 1M HCl (3 x 5 ml).

Method C: The reaction mixture was washed with brine, dried over MgSO₄ and concentrated under reduced pressure. The crude solid was purified by dry column vacuum chromatography (DCVC) using gradient elution's of DCM/EtOAc (100:0 to 85:15).

***N,N'*-bis[3,4-bis(trifluoromethyl)phenyl]urea (1)**

Purified by method B. Yield: 0.172 g, 32%; Melting point = 221-222°C. ¹H NMR: (500 MHz, DMSO-*d*₆) δ 9.76 (s, 2H), 8.22 (s, 2H), 7.95 (d, *J* = 8.5 Hz, 2H), 7.89 (d, *J* = 9). ¹³C NMR: (125 MHz, DMSO-*d*₆) δ 152.1 (1C), 143.5 (2C), 129.5 (q, *J* = 6 Hz, 2C), 127.0 (q, *J* = 34 Hz, 2C), 123.1 (q, *J* = 271 Hz, 2C), 122.7 (q, *J* = 272 Hz, 2C), 118.8 (q, *J* = 33 Hz, 2C), 117.2 (q, *J* = 7 Hz, 2C). HRMS (ESI) *m/z* [M+H]⁺ calcd for C₁₇H₉F₁₂N₂O 485.0518, found 485.0512.

***N,N'*-bis[4-(trifluoromethylsulfonyl)phenyl]urea (2)**

Purified by method B. Yield: 0.120 g, 25%; Melting point = 304-306°C. ¹H NMR: (500 MHz, DMSO-*d*₆) δ 9.91 (s, 2H), 8.06 (d, *J* = 9.0 Hz, 4H), 7.90 (dt, *J* = 9.0, 2.5 Hz, 4H). ¹³C NMR: (125 MHz, DMSO-*d*₆) δ 151.7 (1C), 147.7 (2C), 132.5 (4C), 120.8 (2C), 119.6 (q, *J* = 324 Hz, 2C), 118.9 (4C). HRMS (ESI) *m/z* [M+H]⁺ calcd for C₁₅H₁₁F₆N₂O₅S₂ 477.0008, found 477.0002.

***N,N'*-bis[3-chloro-5-(trifluoromethyl)phenyl]urea (3)**

Purified by method B. Yield: 0.273 g, 56%; Melting point = 210-211°C. ¹H NMR: (500 MHz, DMSO-*d*₆) δ 9.53 (s, 2H), 7.84 (s, 2H), 7.83 (s, 2H), 7.42 (s, 2H). ¹³C NMR: (125 MHz, DMSO-*d*₆) δ 152.2 (1C), 141.6 (2C), 134.2 (2C), 131.1 (q, *J* = 32 Hz, 2C), 123.3 (q, *J* = 271 Hz, 2C), 121.6 (2C), 118.3 (2C), 113.5 (q, *J* = 4 Hz, 2C). HRMS (ESI) *m/z* [M+H]⁺ calcd for C₁₅H₉Cl₂F₆N₂O 416.9991, found 416.9985.

***N,N'*-bis[3,5-dichlorophenyl]urea (SR4)**

Purified by method A. Yield: 0.190 g, 35%. ¹H and ¹³C NMR, mp, and HRMS are in agreement with previously reported data.^{19,34}

***N,N'*-bis[4(methylsulfonyl)phenyl]urea (5)**

Purified by method A. Yield: 0.100 g, 20%, Melting point = 301-303°C. ¹H and ¹³C NMR and HRMS are in agreement with previously reported data.³⁵

N,N'-bis[4-chloro-3-(trifluoromethyl)phenyl]urea (6)

Purified by method B. Yield: 0.266 g, 41%; Melting point = 231-232°C. ¹H and ¹³C NMR and HRMS are in agreement with previously reported data.³⁶

N,N'-bis[4-(trifluoromethyl)phenyl]urea (7)

Purified by method C. Yield: 0.211 g, 43%. ¹H and ¹³C NMR, mp, and HRMS are in agreement with previously reported data.³⁷

N,N'-bis(4-acetylphenyl)urea (8)

Reaction volume was increased to 20 ml to accommodate for the low solubility of the **8** carbamoylimidazole intermediate. Purified by method A. Yield: 0.162 g, 33%. ¹H and ¹³C NMR, mp, and HRMS are in agreement with previously reported data.³⁸

N,N'-bis[4-(trifluoromethoxy)phenyl]urea (9)

Purified by method A. Yield: 0.191 g, 36%. ¹H and ¹³C NMR, mp, and HRMS are in agreement with previously reported data.³⁹

N,N'-bis[4-chlorophenyl]urea (10)

Purified by method A. Yield: 0.383 g, 70%, ¹H and ¹³C NMR, mp, and HRMS are in agreement with previously reported data.⁴⁰

N,N'-diphenylurea (11)

Purified by method A. Yield: 0.340 g, 60%, ¹H and ¹³C NMR, mp, and HRMS are in agreement with previously reported data.³⁷

N,N'-bis(3,4-dimethylphenyl)urea (12)

Purified by method A. Yield: 0.363 g, 65%; ^1H and ^{13}C NMR, mp, and HRMS are in agreement with previously reported data.⁴⁰

N,N-bis(3,4-dimethylphenyl)urea (13)

Purified by method A. Yield: 0.212 g, 42%; ^1H and ^{13}C NMR, mp, and HRMS are in agreement with previously reported data.⁴¹

N,N-bis(4-methoxyphenyl)urea (14)

Purified by method A. Yield: 0.265 g, 48%, ^1H and ^{13}C NMR, mp, and HRMS are in agreement with previously reported data.⁴⁰

Cell-based assays

General

Human MDA-MB-231 breast cancer cells were obtained from ATCC. Cells were cultured in Dulbecco's Modified Eagle Medium containing 10% (v/v) fetal bovine serum (Thermo Fischer Scientific) and 1% (v/v) penicillin/streptomycin (Sigma-Aldrich), at 37°C in a humidified atmosphere of 5% CO_2 . Confluent cells (80-90%) were harvested with trypsin/EDTA after washing in Dulbecco's phosphate-buffered saline (dPBS, Sigma-Aldrich). Cells were treated with various concentrations of the test compounds in DMSO (final concentration 0.1% v/v); control cells were treated with DMSO alone.

JC-1

MDA-MB-231 cells were seeded in triplicate in black wall 96 well plates (1.5×10^4 cells per well) in complete media 24 h before treatment. Media was removed and cells were treated with various drug concentrations in complete media and incubated for one hour. Cells were incubated with JC-1 in media for 20 minutes, washed with dPBS and read using a Tecan Infinite M1000 Pro plate reader to evaluate red (535 nm) and green (595 nm) fluorescence using

excitation wavelengths of 485 and 535 nm respectively (JC-1 Mitochondrial Membrane Potential Assay Kit; Cayman Chemical).

Seahorse Xfe24 Mito Stress Test

Mitochondrial function was measured by determining the oxygen consumption rate (OCR) of cells with a Seahorse XF24 extracellular flux analyzer (Seahorse Bioscience) according to the manufacturer's protocol. MDA-MB-231 cells were seeded in Seahorse XF24 well cell culture microplates (2.0×10^4 cells per well) in complete media, allowed to adhere for three hours at room temperature and incubated overnight. Well media was replaced with 500 μ L XF media (1 mM pyruvate, 2 mM glutamine and 10mM glucose Seahorse XF DMEM medium, pH 7.4 with 5 mM HEPES), placed in a non-CO₂ incubator (37°C, humidified) for one hour, and then OCR was measured utilising an XF Cell Mito Stress Test Kit (Seahorse Bioscience, MA, USA). Oligomycin (final concentration 1 μ M), FCCP (final concentration 0.5 μ M) or test compounds (final concentration 5 μ M or 10 μ M), and rotenone/antimycin A (final concentrations 0.5 μ M each) were added to the sensor cartridge, and the OCR was measured using a modified cycling program on Agilent Seahorse Wave Desktop software.

Intracellular ATP

MDA-MB-231 cells were seeded in triplicate in 96 well plates (1.0×10^4 cells per well) in complete media 24 h before treatment. At different timepoints, media was removed and cells were treated with test compounds (5 μ M) and incubated for the duration of the experiment. Cells were incubated with CellTiter-Glo® 2.0 in complete media, mixed on an orbital shaker for two minutes, left at room temperature in dark conditions for 10 minutes and luminescence was read on a Tecan Infinite M1000 Pro plate reader (CellTiter-Glo® 2.0 Luminescent Cell Viability Assay).

LDH release

MDA-MB-231 cells were seeded in triplicate in 96 well plates (1.0×10^4 cells per well) in complete media 24 h before treatment. Media was removed and cells were treated with test compounds ($5 \mu\text{M}$) or vehicle control and incubated for 8 hours. Well media was homogenized gently, sampled, diluted in LDH storage buffer and stored at -20°C , including wells containing vehicle control treated with 0.2% (v/v) Triton X-100 (Sigma-Aldrich) and incubated for 15 minutes prior to sampling to obtain a maximum LDH release value. Samples were thawed, incubated with LDH detection reagent in a black wall plate at room temperature for one hour and luminescence was measured on a Tecan infinite M1000 Pro plate reader (LDH-Glo™ Cytotoxicity Assay, Promega).

MTS

MDA-MB-231 cells were seeded in triplicate in 96 well plates (3.5×10^3 cells per well) in complete media and incubated for 24 h before treatment. Media was removed and cells were treated with various drug concentrations in complete media and incubated for 72 hours. Cells were then incubated with CellTiter MTS 96® Aqueous MTS Reagent Powder (Promega) and phenazine ethosulphate (Sigma-Aldrich) in dark conditions for approximately three hours. Absorbance of each well at 490 nm was measured using Tecan Infinite M1000 Pro plate reader to evaluate cell viability (CellTiter 96® Aqueous Non-Radioactive Cell Proliferation Assay, Promega).

Statistical Analysis

All data are expressed throughout as means \pm SEM from three independent experiments (N=3). Dose-response curves were constructed using log(inhibitor) vs response, variable slope (4 parameters) non-linear regressions on GraphPad Prism 8. Equation: $Y = \text{Bottom} + (\text{Top} - \text{Bottom}) / (1 + 10^{((\text{LogIC50} - X) * \text{HillSlope}))}$. Absolute IC50 concentrations were interpolated from these normalized curves (data normalized to DMSO vehicle control) with the top constrained to 100%. ATP and Apoptosis data are expressed as mean percentage of time-

matched DMSO control. (*) $P < 0.05$, (**) $P < 0.01$, (***) $P < 0.001$ versus time-matched control by two-way ANOVA with Dunnett's multiple comparison test. Seahorse data normalized to baseline OCR prior to oligomycin addition.

Supporting Information

Supporting Information available: This material is available free of charge via the internet at <http://pubs.acs.org>.

HPTS proton transport assay protocol, bisaryl urea absolute quantitative ^1H NMR purity determination, representative JC-1 / MTS dose-response curves, ATP assay data distribution, LDH release cytotoxicity assay, bisaryl urea ^1H and ^{13}C NMR spectra, HPTS dose-response and Hill Analyses

Acknowledgments

The author acknowledges H. Macdermott-Opeskin for his assistance in preparing the manuscript. D. McNaughton and P. Gale acknowledge and pay respect to the Gadigal people of the Eora Nation, the traditional owners of the land on which we research, teach, and collaborate at the University of Sydney. P. Gale thanks the University of Sydney and the Australian Research Council (DP200100453) for funding.

*Correspondence:

Dr Tristan Rawling, School of Mathematical and Physical Sciences, Faculty of Science, University of Technology Sydney, Ultimo, NSW 2007, Australia. Tel: (61-2)-9514-7956, Email: Tristan.Rawling@uts.edu.au

References

1. Fulda, S.; Galluzzi, L.; and Kroemer, G. (2010) Targeting mitochondria for cancer therapy, *Nat. Rev. Drug Discov.* 9 (6), 447-464.
2. Cooper, G. M. (2000) The Mechanism of Oxidative Phosphorylation, *The Cell: A Molecular Approach*. 2nd edition.
3. Lodish, H.; Berk, A.; Zipursky, S. L.; Matsudaira, P.; Baltimore, D.; and Darnell, J. (2000) Electron Transport and Oxidative Phosphorylation, *Molecular Cell Biology*. 4th edition.
4. Papa, S.; Martino, P. L.; Capitanio, G.; Gaballo, A.; De Rasmio, D.; Signorile, A.; and Petruzzella, V. (2012) The oxidative phosphorylation system in mammalian mitochondria, *Adv. Exp. Med. Biol.* 942, 3-37.
5. Weinberg, S. E.; and Chandel, N. S. (2015) Targeting mitochondria metabolism for cancer therapy, *Nat. Chem. Biol.* 11 (1), 9-15.
6. Gogvadze, V.; Orrenius, S.; Zhivotovsky, B. (2008) Mitochondria in cancer cells: what is so special about them? *Trends Cell Biol.* 18 (4), 165-173.
7. Bonnet, S.; Archer, S. L.; Allalunis-Turner, J.; Haromy, A.; Beaulieu, C.; Thompson, R.; Lee, C. T.; Lopaschuk, G. D.; Puttagunta, L.; Bonnet, S.; et al. (2007) A Mitochondria-K⁺ Channel Axis Is Suppressed in Cancer and Its Normalization Promotes Apoptosis and Inhibits Cancer Growth, *Cancer Cell* 11 (1), 37-51.
8. Heerdt, B. G.; Houston, M. A.; Augenlicht, L. H. (2005) The intrinsic mitochondrial membrane potential of colonic carcinoma cells is linked to the probability of tumor progression. *Cancer Res.* 65 (21), 9861-9867.
9. Childress, E. S.; Alexopoulos, S. J.; Hoehn, K. L.; Santos, W. L. (2018) Small Molecule Mitochondrial Uncouplers and Their Therapeutic Potential. *J. Med. Chem.* 61 (11), 4641-4655.

10. Ripoll, C.; Roldan, M.; Contreras-Montoya, R.; Diaz-Mochon, J. J.; Martin, M.; Ruedas-Rama, M. J.; Orte, A. (2020) Mitochondrial pH Nanosensors for Metabolic Profiling of Breast Cancer Cell Lines. *Int. J. Mol. Sci.* 21 (10), 3731.
11. Benz, R.; McLaughlin, S. (1983) The molecular mechanism of action of the proton ionophore FCCP (carbonylcyanide p-trifluoromethoxyphenylhydrazone). *Biophys. J.* 41 (3), 381-98.
12. Shrestha, R.; Johnson, E.; Byrne, F. L. (2021) Exploring the therapeutic potential of mitochondrial uncouplers in cancer. *Mol. Metab.* 101222-101222.
13. Di Paola, M.; Lorusso, M. (2006) Interaction of free fatty acids with mitochondria: coupling, uncoupling and permeability transition. *Biochim. Biophys. Acta.* 1757 (9-10), 1330-7.
14. Wojtczak, L.; Wieckowski, M. R.; Schönfeld, P. (1998) Protonophoric activity of fatty acid analogs and derivatives in the inner mitochondrial membrane: a further argument for the fatty acid cycling model. *Arch. Biochem. Biophys.* 357 (1), 76-84.
15. Figarola, J. L.; Singhal, J.; Tompkins, J. D.; Rogers, G. W.; Warden, C.; Horne, D.; Riggs, A. D.; Awasthi, S.; Singhal, S. S. (2015) SR4 Uncouples Mitochondrial Oxidative Phosphorylation, Modulates AMP-dependent Kinase (AMPK)-Mammalian Target of Rapamycin (mTOR) Signaling, and Inhibits Proliferation of HepG2 Hepatocarcinoma Cells. *J. Biol. Chem.* 290 (51), 30321-30341.
16. Figarola, J. L.; Weng, Y.; Lincoln, C.; Horne, D.; Rahbar, S. (2012) Novel dichlorophenyl urea compounds inhibit proliferation of human leukemia HL-60 cells by inducing cell cycle arrest, differentiation and apoptosis. *Investig. New Drugs* 30 (4), 1413-1425.
17. Singhal, S. S.; Figarola, J.; Singhal, J.; Leake, K.; Nagaprashantha, L.; Lincoln, C.; Gugiu, G. B.; Horne, D.; Jove, R.; Awasthi, S.; et al. (2012) 1,3-Bis(3,5-dichlorophenyl)

urea compound 'COH-SR4' inhibits proliferation and activates apoptosis in melanoma. *Biochem. Pharmacol.* 84 (11), 1419-1427.

18. Figarola, J. L.; Singhal, J.; Singhal, S.; Kusari, J.; Riggs, A. (2018) Bioenergetic modulation with the mitochondria uncouplers SR4 and Niclosamide prevents proliferation and growth of treatment-I and vemurafenib-resistant melanomas. *Oncotarget* 9 (97).

19. Singhal, S. S.; Figarola, J.; Singhal, J.; Nagaprashantha, L.; Berz, D.; Rahbar, S.; Awasthi, S. (2013) Novel compound 1,3-bis (3,5-dichlorophenyl) urea inhibits lung cancer progression. *Biochem. Pharmacol.* 86 (12), 1664-72.

20. Ho, J.; Zwicker, V. E.; Yuen, K. K. Y.; Jolliffe, K. A. (2017) Quantum Chemical Prediction of Equilibrium Acidities of Ureas, Deltamides, Squaramides, and Croconamides. *J. Org. Chem.* 82 (19), 10732-10736.

21. Wu, X.; Gale, P. A. (2016) Small-Molecule Uncoupling Protein Mimics: Synthetic Anion Receptors as Fatty Acid-Activated Proton Transporters. *J. Am. Chem. Soc.* 138 (50), 16508-16514.

22. Gale, P. A.; Davis, J. T.; Quesada, R. (2017) Anion transport and supramolecular medicinal chemistry. *Chem. Soc. Rev.* 46 (9), 2497-2519.

23. Davis, J. T.; Gale, P. A.; Quesada, R. (2020) Advances in anion transport and supramolecular medicinal chemistry. *Chem. Soc. Rev.* 49 (16), 6056-6086.

24. Blažek Bregović, V.; Basarić, N.; Mlinarić-Majerski, K. (2015) Anion binding with urea and thiourea derivatives. *Coord. Chem. Rev.* 295, 80-124.

25. Amendola, V.; Fabbrizzi, L.; Mosca, L. (2010) Anion recognition by hydrogen bonding: urea-based receptors. *Chem. Soc. Rev.* 39 (10), 3889-3915.

26. Penzo, D.; Tagliapietra, C.; Colonna, R.; Petronilli, V.; Bernardi, P. (2002) Effects of fatty acids on mitochondria: implications for cell death. *Biochim. Biophys. Acta. Bioenerg.* 1555 (1), 160-165.

27. Antonenko, Y. N.; Avetisyan, A. V.; Cherepanov, D. A.; Knorre, D. A.; Korshunova, G. A.; Markova, O. V.; Ojovan, S. M.; Perevoshchikova, I. V.; Pustovidko, A. V.; Rokitskaya, T. I.; et al. (2011) Derivatives of rhodamine 19 as mild mitochondria-targeted cationic uncouplers, *J. Biol. Chem.* 286 (20), 17831-17840.
28. Gilchrist, A. M.; Wang, P.; Carreira-Barral, I.; Alonso-Carrillo, D.; Wu, X., Quesada, R.; and Gale, P. A. (2021) Supramolecular methods: the 8-hydroxypyrene-1,3,6-trisulfonic acid (HPTS) transport assay, *Supramol. Chem.* 1-20.
29. Hansch, C.; Leo, A.; Unger, S. H.; Kim, K. H.; Nikaitani, D.; Lien, E. J. (1973) Aromatic substituent constants for structure-activity correlations. *J. Med. Chem.* 16 (11), 1207-1216.
30. Saggiomo, V.; Otto, S.; Marques, I.; Félix, V.; Torroba, T.; and Quesada, R. (2012) The role of lipophilicity in transmembrane anion transport, *ChemComm.* 48 (43), 5274-5276.
31. Knight, N. J.; Hernando, E.; Haynes, C. J. E.; Busschaert, N.; Clarke, H. J.; Takimoto, K.; García-Valverde, M.; Frey, J. G.; Quesada, R. and Gale, P. A. (2016) QSAR analysis of substituent effects on tambjamine anion transporters, *Chem. Sci.* 7 (2), 1600-1608.
32. Plitzko, B.; and Loesgen, S. (2018) Measurement of Oxygen Consumption Rate (OCR) and Extracellular Acidification Rate (ECAR) in Culture Cells for Assessment of the Energy Metabolism, *Bio. Protoc.* 8 (10), e2850-e2850.
33. Ko, S.-K.; Kim, S. K.; Share, A.; Lynch, V. M.; Park, J.; Namkung, W.; Van Rossom, W.; Busschaert, N.; Gale, P. A.; Sessler, J. L.; et al. (2014) Synthetic ion transporters can induce apoptosis by facilitating chloride anion transport into cells, *Nat. Chem.* 6 (10), 885-892.
34. Ricci, A.; Carra, A.; Rolli, E.; Bertoletti, C.; Morini, G.; Incerti, M.; and Vicini, P. (2004) Effect of Cl-Substitution on Rooting- or Cytokinin-like Activity of Diphenylurea Derivatives, *J. Plant Growth Reg.* 23 (4), 261-268.

35. Marshall, S. R.; Singh, A.; Wagner, J. N.; and Busschaert, N. (2020) Enhancing the selectivity of optical sensors using synthetic transmembrane ion transporters, *ChemComm.* 56 (92), 14455-14458.
36. Denoyelle, S.; Chen, T.; Chen, L.; Wang, Y.; Klosi, E.; Halperin, J. A.; Aktas, B. H.; and Chorev, M. (2012) In vitro inhibition of translation initiation by N,N'-diarylureas—potential anti-cancer agents, *Bioorg. Med. Chem. Lett.* 22 (1), 402-409.
37. Busschaert, N.; Kirby, I. L.; Young, S.; Coles, S. J.; Horton, P. N.; Light, M. E.; and Gale, P. A. (2012) Squaramides as potent transmembrane anion transporters, *Angew. Chem. Int. Ed. Engl.* 51 (18), 4426-4430.
38. Guan, Z.-H.; Lei, H.; Chen, M.; Ren, Z.-H.; Bai, Y.; and Wang, Y.-Y. (2012) Palladium-Catalyzed Carbonylation of Amines: Switchable Approaches to Carbamates and N,N'-Disubstituted Ureas, *Adv. Synth. Catal.* 354 (2-3), 489-496.
39. Wang, M.; Han, J.; Si, X.; Hu, Y.; Zhu, J.; and Sun, X. (2018) Effective approach to ureas through organocatalyzed one-pot process, *Tetrahedron Lett.* 59 (17), 1614-1618.
40. Pfeifer, L.; Engle, K. M.; Pidgeon, G. W.; Sparkes, H. A.; Thompson, A. L.; Brown, J. M.; and Gouverneur, V. (2016) Hydrogen-Bonded Homoleptic Fluoride–Diarylurea Complexes: Structure, Reactivity, and Coordinating Power, *J. Am. Chem. Soc.* 138 (40), 13314-13325.
41. Zhou, S.; Yao, T.; Yi, J.; Li, D.; and Xiong, J. (2013) A Simple and Efficient Synthesis of Diaryl Ureas with Reduction of the Intermediate Isocyanate by Triethylamine, *J. of Chem. Res.* 37 (5), 315-319.

ToC Graphic

